

AIR FLOW AROUND BODIES IN SUBSONIC WIND TUNNEL

LIM FONG KIAW

This report is submitted as partial requirement for the completion of the Bachelor of
Mechanical Engineering (Thermal Fluids) Degree Program

Faculty of Mechanical Engineering
Universiti Teknikal Malaysia Melaka

MAY 2009

DECLARATION

“I hereby, declare this report is resulted from my own research except as cited in the references”

Signature :.....
Author's Name :.....
Date :.....

DEDICATION

To my beloved parents

ACKNOWLEDGEMENT

First and foremost, I would like to take this opportunity to express my heartfelt gratitude to my final year project supervisor, Mr. Shamsul Bahari Bin Azraai, who has graciously offered his time, attention, experience and guidance throughout the completion of project. Many thanks as well to the Faculty of Mechanical Engineering, Universiti Teknologi Malaysia Melaka (UTeM) for the opportunities given and facilities offered. I would also like to extend my thanks to Mr. Hambali Bin Boejang who is the Rapid Prototyping Laboratory Coordinator and Mr. Razmi, who is the technician in the fluid laboratory of Universiti Teknologi Malaysia Melaka (UTeM) for their assistance and explanation of the Rapid Prototyping Machine and Subsonic Wind Tunnel facilities in UTeM. Besides that, I would like to express my sincere appreciation to all the occupants of No. 23, Jalan TU 23, Taman Tasik Utama for their consistent words of wisdom and company throughout the late nights. Finally, I would like to thank each and every individual who either has directly or indirectly helped me in the form of encouragement, advice or kind reminders throughout the efforts of this report.

ABSTRACT

In this study, air flow around bodies in a subsonic wind tunnel is investigated. The investigation focuses on drag force for two slightly different in percentage of camber for the streamlined body based on the existing NACA four-digit series airfoil model. In order to reduce the drag force to get a better performance of airfoil, the drag force was measured and determined through the subsonic wind tunnel test. Computational Fluid Dynamic was used to simulate the external flow analysis on the airfoils and then the prediction of the drag force to validate its simulation result with the experimental result. NACA 2412 and NACA 4412 airfoil geometry profiles and its coordinates were generated from a NACA 4 Digits Series Generator and then designed by using Solidworks software. The airfoil models were made by rapid prototyping to run the wind tunnel tests. The results revealed that NACA 2412 has a better performance due to its smaller drag force compared to NACA 4412. However, NACA 4412 has a greater lift force than the NACA 2412. Moreover, smaller drag had better performance among the others due to its less fuel consumption during cruising speed.

ABSTRAK

Dalam kajian ini, aliran udara di sekitar objek di dalam sebuah terowong angin subsonik dikaji. Siasatan menumpukan daya seretan ke atas dua model yang bercirikan garisan arus yang berbeza sedikit dari segi peratusan kelengkungan dengan berdasarkan bentuk airfoil NACA bersiri empat digit yang sedia ada. Dengan tujuan mengurangkan daya seretan untuk mendapat satu prestasi yang lebih baik, daya seretan telah disukat dan ditentukan melalui ujian terowong angin subsonik. Kaedah dinamik bendalir berbantuan komputer adalah digunakan untuk menganalisis aliran udara luar pada bentuk airfoil dan kemudian ramalan menyahihkan daya seretan daripada keputusan simulasi dengan eksperimen. Bentuk geometri dan koordinat-koordinat airfoil NACA 2412 dan NACA 4412 dihasilkan daripada *NACA 4 Digits Series Generator* dan direka bentuk kemudian dengan menggunakan perisian *Solidworks*. Model berbentuk airfoil dihasilkan dengan menggunakan *rapid prototyping* untuk mengendalikan ujian terowong angin. Keputusan menunjukkan bahawa NACA 2412 mempunyai prestasi yang lebih baik kerana daya seretan lebih kecil berbanding dengan NACA 4412. Bagaimanapun, NACA 4412 mempunyai daya angkat yang lebih besar daripada NACA 2412. Lagipun, seretan lebih kecil mempunyai prestasi yang lebih baik di antara yang lain akibat kurang penggunaan bahan api.

LIST OF CONTENTS

CHAPTER	TOPIC	PAGE
	DECLARATION	ii
	DEDICATION	iii
	ACKNOWLEDGEMENT	iv
	ABSTRACT	v
	ABSTRAK	vi
	LIST OF CONTENTS	vii
	LIST OF TABLES	xi
	LIST OF FIGURES	xii
	LIST OF SYMBOLS	xiv
	LIST OF APPENDICES	xvi
1.0	INTRODUCTION	1
	1.1 Background Study	1
	1.2 Problem Statement	4
	1.3 Objectives	4
	1.4 Scopes	4

CHAPTER	TOPIC	PAGE
2.0	LITERATURE REVIEW	5
2.1	Background about Airfoils	5
2.2	Airfoils Nomenclature	7
2.3	Previous Studies of Air Flow on Bodies and Airfoils	9
2.4	Computational Fluid Dynamics	10
	2.4.1 Applications of Computational Fluid Dynamics	11
	2.4.2 Advantages of Computational Fluid Dynamics	12
	2.4.3 Disadvantages of Computational Fluid Dynamics	12
2.5	Wind Tunnel	13
	2.5.1 Subsonic Wind Tunnel	13
2.6	Drag and Related Equations	14
3.0	METHODOLOGY	18
3.1	Introduction	18
3.2	Experimental Setup	19
	3.2.1 Description of Subsonic Wind Tunnel	19
	3.2.2 Experimental Procedures	21
3.3	CFX Computational Fluid Dynamics	23
	3.3.1 ANSYS CFX 10.0 Computational Fluid Dynamic Software	23
	3.3.2 CFD Simulation Flow Chart	25
	3.3.3 CFD Simulation	26

CHAPTER	TOPIC	PAGE
4.0	RESULTS AND DISCUSSIONS	30
4.1	Introduction	30
4.2	Simulation Results	30
4.2.1	Lift and Drag Force at Different Angle of Attack	32
4.2.1.1	Lift and drag force with different angle of attack at air velocity of 10 m/s	32
4.2.1.2	Lift and drag force with different angle of attack at air velocity of 30 m/s	33
4.2.2	Lift and Drag Force with Different Angle of Attack at Various Air Velocities	34
4.2.3	Velocity and Pressure Profiles at Various Air Velocity and Angle of Attack	36
4.2.3.1	Velocity and pressure profiles at air velocity of 10 m/s	36
4.2.3.2	Velocity and pressure profiles at air velocity of 30 m/s	39
4.3	Experimental Results	42
4.3.1	Lift and Drag Force at Different Angle of Attack	44
4.3.1.1	Lift and drag force with different angle of attack at air velocity of 10 m/s	44

CHAPTER	TOPIC	PAGE
	4.3.1.2 Lift and drag force with different angle of attack at air velocity of 30 m/s	45
	4.3.2 Lift and Drag Force with Different Angle of Attack at Various Air Velocities	46
4.4	Comparison between Simulation and Experimental Results	48
	4.4.1 Comparison between Simulation and Experimental Results for Lift and Drag Force with Different Angle of Attack at 30 m/s	50
	4.4.1.1 Discussion on Factors Affecting the Results of Lift and Drag	51
5.0	CONCLUSION AND RECOMMENDATIONS	53
	5.1 Conclusion	53
	5.2 Recommendations	54
	REFERENCES	55
	BIBLIOGRAPHY	58
	APPENDIX A	59
	APPENDIX B	64
	APPENDIX C	66
	APPENDIX D	69
	APPENDIX E	72
	APPENDIX F	76

LIST OF TABLES

NO.	TITLE	PAGE
3.1	Simulation feature and details	28
3.2	Various air inlet velocity settings for CFD simulation	29
4.1	Simulation Results for NACA 2412 and NACA 4412	31
4.2	Experimental Results or NACA 2412 and NACA 4412	43
4.3	Percentages error of lift and drag force for NACA 2412 and NACA 4412	49

LIST OF FIGURES

NO.	TITLE	PAGE
1.1	Drag coefficients of blunt and streamlined body (Source: Munson <i>et al.</i> (2006))	2
1.2	Drag coefficients of various bodies (Source: http://www.centennialofflight.gov)	3
2.1	Phillips Patented Aerocurves – 1884 and 1891 (Source: http://www.desktopaero.com/appliedaero/airfoils1/airfoilhistory.html)	6
2.2	Airfoils nomenclature (Source: Ress. (1962))	7
2.3	Schematic diagram of closed circuit subsonic wind tunnel (Source: http://en.wikipedia.org/wiki/Subsonic_and_transonic_wind_tunnel#Subsonic_tunnel)	14
2.4	Schematic diagram of opened circuit subsonic wind tunnel (Source: http://en.wikipedia.org/wiki/Subsonic_and_transonic_wind_tunnel#Subsonic_tunnel)	14
3.1	Schematic drawing of airfoils. (a) NACA 2412. (b) NACA 4412	19
3.2	Subsonic Wind Tunnel, Downstream Fan in UTeM (Source: http://www.essom.com/productslist.php?p_id=157)	20
3.3	Schematic diagram of Subsonic Wind Tunnel	21
3.4	Displays the oncoming wind direction as well as angle of attack	22
3.5	CFD Simulation Flow Chart	25
3.6	Boundary Conditions of CFD Simulation	27

NO.	TITLE	PAGE
3.7	Four planes of wind tunnel test section as FreeWalls Boundaries	28
4.1	Forces with air velocity of 10 m/s at different angle of attack	33
4.2	Forces with air velocity of 30 m/s at different angle of attack	34
4.3	Forces versus angle of attack at various air velocities	35
4.4	Velocity and pressure profiles at air velocity of 10 m/s and the angle of attack, $\alpha = 0^\circ$	37
4.5	Velocity and pressure profiles at air velocity of 10 m/s and the angle of attack, $\alpha = 20^\circ$	38
4.6	Velocity and pressure profiles at air velocity of 10 m/s and the angle of attack, $\alpha = 50^\circ$	39
4.7	Velocity and pressure profiles at air velocity of 30 m/s and the angle of attack, $\alpha = 0^\circ$	40
4.8	Velocity and pressure profiles at air velocity of 30 m/s and the angle of attack, $\alpha = 20^\circ$	41
4.9	Velocity and pressure profiles at air velocity of 30 m/s and the angle of attack, $\alpha = 50^\circ$	42
4.10	Forces with air velocity of 10 m/s at different angle of attack	45
4.11	Forces with air velocity of 30 m/s at different angle of attack	46
4.12	Forces versus angle of attack at various air velocities	47
4.13	Comparison between experimental and simulation results at air velocity of 30 m/s.	51

LIST OF SYMBOLS

A	=	Reference/characteristic area of the body (planform area for airfoils)
A_v	=	Wetted area of the body
a	=	Speed of sound (m/s)
b	=	Wing span
C_D	=	Drag coefficient
C_L	=	Lift coefficient
C_{Dp}	=	Pressure or form drag coefficient
C_{Dv}	=	Viscous or skin friction drag coefficient
c	=	Mean chord length
F_D	=	Total drag force on the body
F_L	=	Lift force on the body
L	=	Characteristic length chord length (m)
M	=	Mach number
R	=	Specific gas constant, which equal to 287J/kg/K
Re	=	Reynolds number
T_c	=	Atmospheric temperature in degree Celcius ($^{\circ}C$)
U	=	Free stream velocity (m/s)
V	=	Mean fluid velocity (m/s)

Greek letters

ρ	Density of the fluid (kg/m ³)
μ	Fluid dynamic viscosity (Pa·s or N·s/m ²)
ν	Fluid kinematic viscosity (defined as $\nu = \mu / \rho$) (m ² /s)
k	Specific heat ratio, which is usually equal to 1.4
α	Angle of attack

Acronyms

CAD	Computer-Aided-Design
CFD	Computational Fluid Dynamics
NACA	National Advisory Committee on Aeronautics (USA)
NASA	National Aeronautics and Space Administration

LIST OF APPENDICES

NO.	TITLE	PAGE
A	Sample Calculations for Similarity	59
B	NACA 4 Digits Series Generator Program	64
C	NACA 2412 and NACA 4412 Airfoils Drawings	66
D	Specifications of Subsonic Wind Tunnel	69
E	Simulation Results for Air Velocity of 20 m/s	72
F	Experimental Results at Air Velocity of 20 m/s	76

CHAPTER 1

INTRODUCTION

1.1 Background Study

According to Finnemore and Franzini (2002), a body that immersed in a moving fluid, experiences a resultant force due to the interaction between the body and the completely surrounded fluid. This is one of the flow classifications of aerodynamics (which is a branch of dynamics concerned with studying the air motion), named as external flow as well as internal flow. The forces arising from that relative motion are known as drag and lift which is resolved along the tangential and the normal direction to the surface respectively.

Based on Cengel and Cimbala (2006), a drag force which can be divided into two components: frictional drag and pressure drag, is produced when a body moving through a fluid or a moving fluid flow throughout a body. Frictional drag comes from friction between the fluid and the surfaces over which it is flowing and it is associated with the development of boundary layers, and it scales with Reynolds number. Frictional drag is the component of the wall shear force in the flow direction and thus it depends on the orientation of body. The pressure drag which is also called form drag, is proportional to the frontal area and the pressure difference acting to the front and the back of the immersed body. The pressure drag is the most significant when the fluid velocity is too high and thus there is a separated region (low pressure region) occurs.

However, from the statement (Finnemore et al. 2002) mention that the drag force can be reduced by streamlining a body. By delaying the boundary layer separation, the pressure drag is reduced and the frictional drag is increased by increasing the surface area. For the streamlined body, the drag is almost entirely due to friction drag by which will only increase the surface area and thus the total drag (sum of the friction drag and pressure drag). By other means that the bodies shape can be classified into blunt/bluff body (sphere, building and etc.) and streamlined body (aerofoil, racing car and etc.) which have a different in drag force and thus its drag coefficient. Some instances of drag coefficients of blunt and streamlined body versus Reynolds number is shown as in Figure 1.1 and the drag coefficients of various bodies as shown in Figure 1.2.

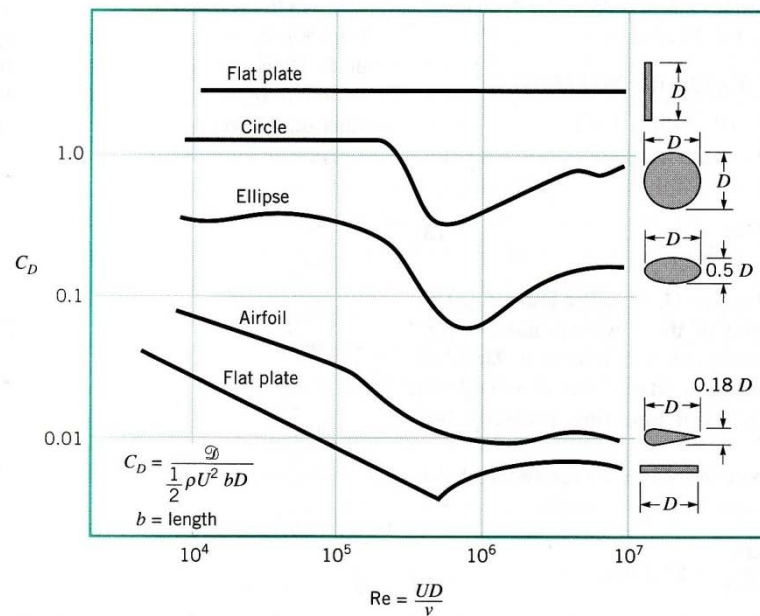


Figure 1.1: Drag coefficients of blunt and streamlined body versus Reynolds number
(Source: Munson *et al.* (2006)).

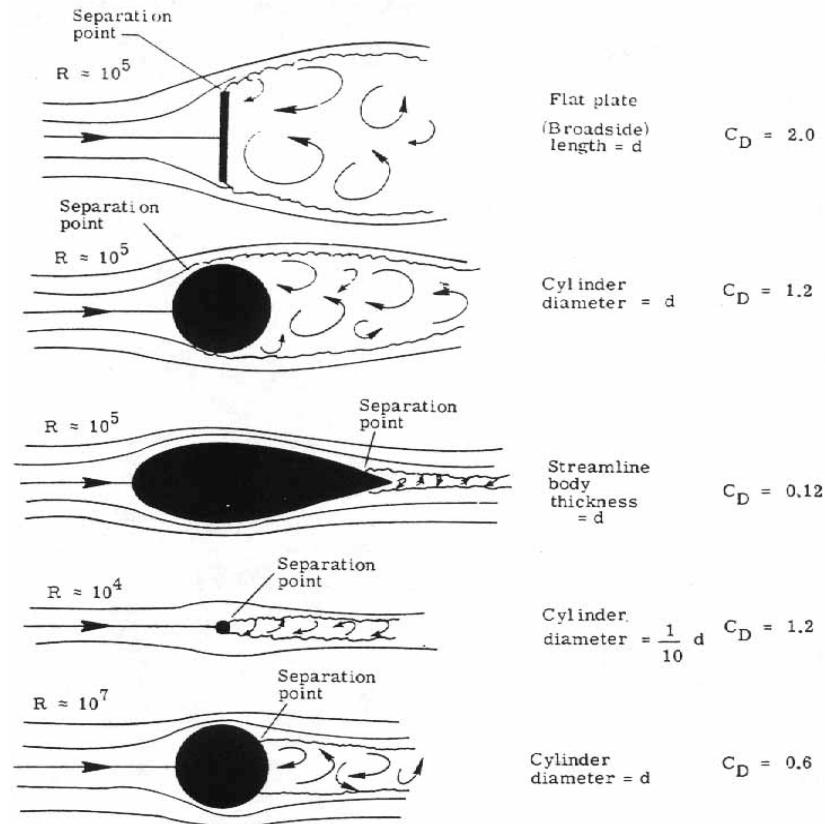


Figure 1.2: Drag coefficients of various bodies

(Source: <http://www.centennialofflight.gov>)

Furthermore, the drag and lift coefficient are primarily function of the shape of the body, but they also may depends on the Reynolds number, the Mach number and the surface roughness. From Finnemore and Franzini (2002), for a subsonic flow (low speed flow), a streamlined body which has a rounded-nose and a long, tapered afterbody (its streamlining must be given to the rear end or downstream part as well as to the front), produces the least disturbance.

In addition to that, airfoil (which is known as streamlined body) are widely used and applied for aircraft fuselage or wings, helicopter rotor, turbine blade, and vehicles shape due to different thickness and camber of the airfoils since different application required different airfoil characteristics and properties.

1.2 Problem Statement

To solve the drag force problem on such bodies like turbine blade, aircraft wings or vehicles, it is important that the drag should be reduced since the increase in drag force will tend to affect the performance to become lower due to larger air resistance and also will increase its fuel consumption. Thus, the Computational Fluid Dynamics will be utilized to overcome this higher drag force problem and then to get a better result on design and optimize its performance. This simulation result also will be validated with the wind tunnel test result.

1.3 Objectives

The objectives of this project are to determine the drag force around streamlined body. To achieve this aim, experiment was conducted on two prototype airfoil models. In addition to that, the experiment was performed to validate the simulation data that was developed using CFX software.

1.4 Scopes

The investigation had been focused on drag force for a two slightly different in percentage of camber for the streamlined body. The streamlined body that based on the existing aerofoil models had been generated. After that, the experimental work with a Subsonic Wind Tunnel is set-up to measure the drag force for both streamlined body. The models had been simulated by using Computational Fluid Dynamics and the rapid prototyping for the models had been done. Compare both results for the airfoil models for a certain velocity at different angle of attack.

CHAPTER 2

LITERATURE REVIEW

2.1 Background about Airfoils

In the late 1800's, the earliest work on the development of airfoil sections had been started. It was known that flat plates may produce lift at an angle of incidence (which is also named as angle of attack). However, some suspected that shapes with a curvature would produce more lift and more efficient due to its shape resembled to the bird wings. In 1884, a series of airfoil shapes as shown in Figure 2.1, had been altered by H.F. Philips (1845-1926) after the earliest wind tunnel testing in which the artificial of air produced from a steam jet in a wooden trunk or conduit. In 1893, he constructed a large device (sustainers which is also known as airfoils) for the effective lift testing. According to Octave Chanute in 1893, the success and failure of a flying machine will depend upon the sustaining effect between a plane and a curve surface to get a maximum lift.

However, Otto Lilienthal (1848-1896) also had the same ideas with Octave Chanute at that time (1893). He tested the airfoils on a 7 m diameter “whirling machine” due to the shapes of wings measured. After several experiments with different nose radii and thickness distributions that had been done by Lilienthal, he believed that the wing curvature or camber played a main rule for a successful flight. He had been called as the world's first true aviator as a result of his hang gliders and the great enthusiasm generated even though he built no powered aircraft. After that, the Wright Brothers closely

resembled Lilienthal's thin and highly cambered sections to do some of the earliest research on the most effective airfoil (which is a curvature or camber of wing). At an extremely low Reynolds number, such sections behave much better than thicker ones. But there was some of the first airplanes were biplanes because of the wrong belief that efficient airfoils had to be thin and highly cambered.

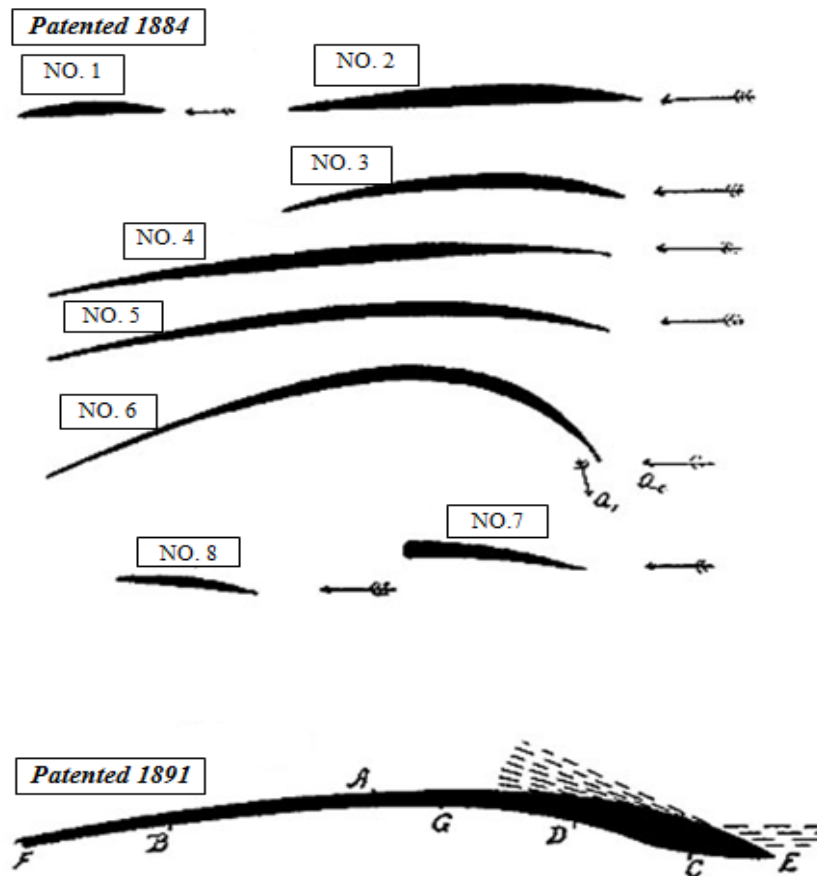


Figure 2.1: Phillips Patented Aerocurves – 1884 and 1891

(Source: <http://www.desktopaero.com/appliedaero/airfoils1/airfoilhistory.html>)

Over the next decade, the use of such sections gradually decreased. In the early 1920's, the NACA had used the Clark Y and Gottingen 398 which are successful sections, as the basic for a family of sections tested. In 1933, NACA issued its monumental Technical Report No. 460, "The Characteristics of 78 Related Airfoil Sections from Tests in the Variable-Density Wind Tunnel." This investigation of a large group of related airfoils was made at a large value of the Reynolds Number which was

made to provide data that may be directly employed for a rational choice of the most suitable airfoil section for a given application. Thus, the NACA airfoils became widely used, for example, the NACA 2412 continued in use on some light aircrafts more than half a century later (Jacobs *et al.* 1933). In 1939, the first laminar flow airfoil sections which had extremely low drag and achieved a lift drag ratio of about 300 had been designed and tested by Eastman Jacobs at NACA in Langley.

Nowadays, most of the airfoils are normally designed especially for their intended application, such as the wing of aircraft, shape for sail or blade of a propeller, rotor or turbine.

2.2 Airfoils Nomenclature

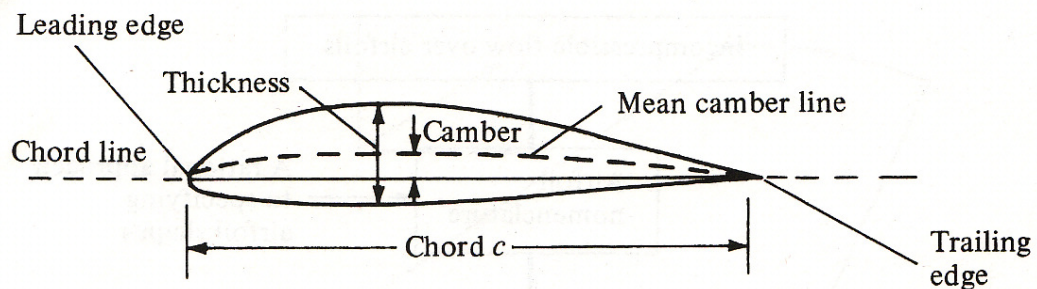


Figure 2.2: Airfoils nomenclature

(Source: Ress. (1962))

The subsonic flight airfoils have a characteristics shape with a rounded leading edge and then followed by a sharp trailing edge, often with asymmetric camber. Consider the airfoil sketched in Figure 2.2, the mean camber line is the locus of points halfway between the upper and lower surface as measured perpendicular to the mean camber line itself.

The leading and trailing edges are the most forward and rearward point of the mean camber line respectively. The straight line connecting the leading and trailing edges is the chord line of the airfoil. The precise distance from the leading to the trailing edge measured along the chord line is simply designated the chord c of the airfoil. The camber is the maximum distance between the mean camber line and the chord line, measured perpendicular to the chord line. The thickness is the distance between the upper and lower surfaces, also measured perpendicular to the chord line. The shape of all standard NACA airfoils are generated by specifying the shape of the mean camber line and then wrapping a specified symmetrical thickness distribution around the mean camber line (Aderson, 2001).

The NACA identified different airfoil shapes with a logical numbering system. However there are several families of NACA airfoils, such as “four-digit” series, “five-digit” series, “6-series”, “7-series” and “8-series”. The six, seven and even eight series were designed to highlight some aerodynamic characteristic.

The first family of NACA airfoils which is developed in 1930s was the “4-digit” (NACA XXXX) series and it means that the first digit expresses the camber in percent chord, the second digit gives the location of the maximum camber point in tenths of chord and finally the last two digits give the thickness in percent chord. For example, 4412 has maximum of 4% of chord located at 40% chord back from the leading edge and is 12% thick while 0006 is a symmetrical section of 6% thickness.